Contribution of reactive oxygen species to cerebral amyloid angiopathy, vasomotor dysfunction, and microhemorrhage in aged Tg2576 mice

Byung Hee Han[a,b,1], Meng-liang Zhou[a,1,2], Andrew W. Johnson[a], Itender Singh[a,b], Fan Liao[c], Ananth K. Vellimana[a], James W. Nelson[a], Eric Milner[a], John R. Cirrito[b,c], Jacob Basak[c], Min Yoo[a], Hans H. Dietrich[a,b], David M. Holtzman[b,c,d], and Gregory Joseph Zipfel[a,b,c,3]

Departments of [a]Neurological Surgery, [c]Neurology, and [d]Developmental Biology, and [b]Hope Center for Neurological Disorders, Washington University School of Medicine, St. Louis, MO 63110

Cerebral amyloid angiopathy (CAA) is characterized by deposition of amyloid β peptide (Aβ) within walls of cerebral arteries and is an important cause of intracerebral hemorrhage, ischemic stroke, and cognitive dysfunction in elderly patients with and without Alzheimer's Disease (AD). NADPH oxidase-derived oxidative stress plays a key role in soluble Aβ-induced vessel dysfunction, but the mechanisms by which insoluble Aβ in the form of CAA causes cerebrovascular (CV) dysfunction are not clear. Here, we demonstrate evidence that reactive oxygen species (ROS) and, in particular, NADPH oxidase-derived ROS are a key mediator of CAA-induced CV deficits. First, the NADPH oxidase inhibitor, apocynin, and the nonspecific ROS scavenger, tempol, are shown to reduce oxidative stress and improve CV reactivity in aged Tg2576 mice. Second, the observed improvement in CV function is attributed both to a reduction in CAA formation and a decrease in CAA-induced vasomotor impairment. Third, anti-ROS therapy attenuates CAA-related microhemorrhage. A potential mechanism by which ROS contribute to CAA pathogenesis is also identified because apocynin substantially reduces expression levels of ApoE—a factor known to promote CAA formation. In total, these data indicate that ROS are a key contributor to CAA formation, CAA-induced vessel dysfunction, and CAA-related microhemorrhage. Thus, ROS and, in particular, NADPH oxidase-derived ROS are a promising therapeutic target for patients with CAA and AD.

Alzheimer's disease | cerebral amyloid angiopathy | reactive oxygen species | NADPH oxidase | vasomotor dysfunction

Cerebral amyloid angiopathy (CAA) is characterized by amyloid deposition within walls of leptomeningeal and cortical arterioles. Among the several types of amyloid proteins causing CAA, fibrillar amyloid β (Aβ) is by far the most common (1). This pathological form of Aβ is also the major constituent of neuritic plaques in patients with Alzheimer's disease (AD) (2). Aβ is a 39- to 43-amino acid peptide that is produced from the amyloid precursor protein (APP) via sequential proteolytic cleavage processed by β- and γ-secretases (3, 4). $A\beta_{40}$ is the predominant Aβ species present in CAA whereas $A\beta_{42}$ is the major Aβ species present in neuritic plaques. CAA is a very common disorder, pathologically affecting about one-third of all elderly patients (>60 y of age) and about 90% of patients with AD (5, 6). CAA is a well-recognized cause of intracerebral hemorrhage (7, 8). It is also a major contributor to ischemic stroke and dementia (2, 9–12)—two conditions in which CAA-induced impairment in cerebral arteriole function is likely to play a fundamental role (13).

Multiple lines of evidence indicate that soluble Aβ monomers and insoluble Aβ fibrils in the form of CAA cause significant cerebrovascular (CV) impairment. Ex vivo studies with isolated cerebral arterioles show that synthetic $A\beta_{40}$ (and to a lesser degree $A\beta_{42}$) induces direct vessel constriction, enhanced response to vasoconstrictors, and reduced response to vasodilators (14–22).

Similar results have been demonstrated with synthetic $A\beta_{40}$ topically applied to the cerebral cortex (23, 24), results that are generally supported by in vivo studies (20, 23, 25). For example, Iadecola and coworkers have shown that young APP transgenic mice (Tg2576) exposed to elevated levels of $A\beta_{40}$ and $A\beta_{42}$ (but no CAA) have reduced baseline cerebral blood flow (CBF) and decreased CBF responses to topical vasodilators (23, 24, 26). We have shown similar CV deficits in young Tg2576 mice (13). Moreover, we provided the most direct evidence to date that endogenous soluble Aβ plays a causal role in these CV deficits when we found that depletion of soluble Aβ via γ-secretase inhibition restores CV function in young Tg2576 mice (13).

Fibrillar Aβ in the form of CAA produces even greater degrees of CV impairment. Evidence for this notion comes from several experimental studies from different laboratories that show reduced pial arteriole responses (27) and diminished CBF responses (27, 28) to a variety of vasodilatory stimuli in aged APP mice with CAA vs. young APP mice without CAA. Our past work examining pial arteriole function in young vs. aged Tg2576 mice shows similar age-dependent CV deficits (13). Moreover, multiple additional observations from our study show that CAA (and not prolonged exposure to soluble Aβ and/or mutant APP) is the principle cause

Significance

One of the hallmarks of Alzheimer's disease (AD) is cerebral amyloid angiopathy (CAA), which is a strong and independent risk factor for cerebral hemorrhage, ischemic stroke, and dementia. However, the mechanisms by which CAA contributes to these conditions are poorly understood. Results from the present study provide strong evidence that vascular oxidative stress plays a causal role in CAA-induced cerebrovascular dysfunction, CAA-induced cerebral hemorrhage, and CAA formation, itself. They also suggest that NADPH oxidase is the source of this oxidative stress and that strategies to inhibit NADPH oxidase may have therapeutic potential in patients with AD and CAA.

of the severe CV dysfunction noted in aged Tg2576 mice: (*i*) The severity of the vasomotor deficits noted in these mice is dependent on the presence and extent of CAA; (*ii*) even small amounts of CAA are associated with profound vasomotor impairment; and (*iii*) the CV dysfunction noted in CAA-ladened arteries is poorly responsive to depletion of soluble Aβ via γ-secretase inhibition (13).

Regarding the mechanism of soluble Aβ-induced CV deficits, increased reactive oxygen species (ROS) are strongly implicated. Cerebral arterioles exposed to exogenous Aβ$_{40}$ develop significant oxidative stress (29), and various anti-ROS strategies have been shown to improve Aβ$_{40}$-induced vessel dysfunction (16, 23). Similarly, cerebral arterioles of young APP mice producing elevated levels of endogenous Aβ$_{40}$ and Aβ$_{42}$ (but no CAA) display oxidative stress (19), and the CV deficits found in these mice can be attenuated by both genetic and pharmacologic anti-ROS interventions (15, 19, 20, 30). In particular, ROS derived from NADPH oxidase—one of two major sources of ROS in the cerebrovasculature (31–33)—have been implicated (28–30, 34, 35).

Regarding the mechanism of CAA-induced CV deficits, far less is known; however, three recent findings suggest that ROS may play a role. First, CAA-affected vessels were shown to have significantly greater oxidative stress than CAA-free vessels of aged Tg2576 mice (36). Second, genetic knockdown of mitochondrial superoxide dismutase 2 (SOD2)—which increases mitochondria-derived ROS—was shown to exacerbate CAA pathology in aged APP mice (37). Third, genetic depletion of the catalytic subunit Nox2 of NADPH oxidase was shown to reduce oxidative stress and improve CV function in aged Tg2576 mice (28, 35). Importantly, the latter studies did not examine for the presence of CAA, nor did they assess for the effect of CAA on cerebral arteriole function (28, 35). To address this critical knowledge gap, we examined the effect of the NADPH oxidase inhibitor, apocynin, and the nonspecific ROS scavenger, tempol, on CAA-induced CV dysfunction in aged Tg2576 mice. The effect of these agents on CAA formation and CAA-related microhemorrhage was also examined.

Results

Oxidative Stress Is Increased in Brain and Cerebral Arteries of Aged Tg2576 Mice.
To test the possibility that NADPH oxidase-derived ROS are associated with CV dysfunction, we first determined gene expression of Nox isoforms in leptomeningeal arteries isolated from 12-mo-old Tg2576 mice and age-matched WT mice by real-time quantitative PCR (qPCR). We found that the level of Nox2 gene expression was significantly increased in leptomeningeal arteries of aged Tg2576 mice vs. littermate controls whereas the level of other Nox isotype genes remained unchanged between the two groups (Fig. 1*A*). Next, we assessed whether brain and cerebral arteries of aged Tg2576 mice have increased oxidative stress. In agreement with past reports (28, 36, 38), we noted that cerebral arterioles as well as neurons of 15-mo-old Tg2576 mice have increased oxidative stress compared with littermate WT mice, as assessed by immuno-labeling with an antibody specific for 3-nitrotyrosine (a marker for oxidative damage) (Fig. 1*B*). Also in agreement with past reports (20), we noted up-regulation of SOD2 (an oxidative stress-inducible enzyme) in the cortex of aged Tg2576 mice by quantitative PCR and Western blot analyses (Fig. 1 *A* and *C*). Finally, we documented increased dihydroxyethidium (DHE) fluorescence (a direct measure of superoxide) in brain and cerebral vessels of aged PS1APP transgenic mice via multiphoton microscopy (see Fig. S3). Taken together, these data indicate that brain and cerebral arteries of aged APP transgenic mice develop substantial oxidative stress.

Apocynin and Tempol Reduce Oxidative Stress and Restore CV Function in Aged Tg2576 Mice.
To examine whether ROS and, in particular, NADPH oxidase-derived ROS contribute to CAA-induced CV dysfunction, Tg2576 mice were administered the NADPH oxidase inhibitor apocynin (1.5 mM) or the ROS scavenger tempol (1 mM) in drinking water for 10–12 wk beginning at 12 mo of age. First, we assessed whether apocynin and tempol pass the blood–brain barrier (BBB) and reach the brain after oral administration. In vitro assays examining lipophilicity and BBB permeability revealed that both apocynin and tempol were highly permeable to the BBB (Fig. S1). In vivo assays showed that apocynin (39) and tempol (Fig. S2) effectively reach the brain after oral administration in mice. Second, we assessed whether apocynin and tempol reduce the oxidative stress found in aged APP transgenic mice. We documented that apocynin and to a lesser degree tempol reduced the oxidative stress noted in brain parenchyma and cerebral vessels of aged APP transgenic mice as determined by immunolabeling of 3-nitrotyrosine (see Fig. 3*B*), Western immunoblotting of SOD2 (Fig. 1 *B* and *C*), and DHE multiphoton microscopy (Fig. S3). Third, we assessed pial arteriole reactivity to endothelial cell (EC)-dependent vasodilators (acetylcholine), EC-independent vasodilators (SNAP), and EC-independent vasoconstrictors (PGF$_{2\alpha}$) via live cranial window. Using this method of assessing CV function, we confirmed our previous finding (13) that pial arteriole responses were significantly reduced in aged Tg2576 mice compared with littermate WT mice (SNAP- Tg2576 mice, 1.7 ± 0.4% vs. WT mice, 4.6 ± 1.1%; $P =$ 0.008; PGF$_{2\alpha}$-Tg2576 mice, 1.3 ± 0.6% vs. WT mice, 4.0 ± 0.8%; $P = 0.008$; acetylcholine-Tg2576 mice, 0.9 ± 0.4% vs. WT mice, 2.8 ± 0.6%; $P = 0.006$) (Fig. 1 *D–F*). We then determined the effect of anti-ROS treatment on this severe form of CV dysfunction. In apocynin-treated aged Tg2576 mice, CV responses to vasoactive stimuli were substantially improved (SNAP-apocynin, 6.6 ± 0.9% vs. vehicle, 1.7 ± 0.4%; $P < 0.001$; PGF$_{2\alpha}$-apocynin, 3.0 ± 1.2% vs. vehicle, 1.3 ± 0.6%; $P = 0.107$; acetylcholine-apocynin, 2.9 ± 0.9% vs. vehicle, 0.9 ± 0.4%; $P = 0.017$). In tempol-treated aged Tg2576 mice, CV responses to vasoactive stimuli were also significantly enhanced (SNAP-tempol, 4.3 ± 0.9% vs. vehicle, 1.7 ± 0.4%; $P < 0.004$) (Fig. 1 *D–F*). This restoration of CV function in apocynin- and tempol-treated Tg2576 mice could not be attributed to differences between groups in baseline vessel diameters (Fig. S4), body weight (Fig. S4), mean arterial blood pressure (Table S1), or blood levels of pCO$_2$ (Table S1). To examine whether anti-ROS therapy directly modulates vascular cell reactivity, we used an in vitro live microscopic imaging system using cultured rat brain vascular smooth muscle cells (VSMCs). We found that incubation of rat VSMCs with soluble Aβ$_{40}$ led to enhanced KCL-induced VSMC constriction (Fig. S5)—a hypercontractile response that was inhibited by cotreatment with apocynin and to a lesser degree tempol (Fig. S5). In total, these data indicate that there is marked impairment in EC-dependent and VSMC-dependent vascular reactivity in aged Tg2576 mice, that this CV dysfunction is mediated via ROS, and that a principle source of the offending ROS is likely NADPH oxidase.

Apocynin Selectively Decreases CAA Formation.
To explore the potential mechanisms by which anti-ROS therapy reduces CV deficits in aged Tg2576 mice, we visualized CAA and neuritic plaque loads using the congophilic fibrillar amyloid dyes methoxy-X04 (for in vivo imaging of CAA and neuritic plaques) (40), methoxy-X34 (for in situ staining of CAA and neuritic plaques) (40), and resorufin (for in situ staining of CAA alone) (41). Similar to our previous report (13), substantial deposition of CAA and neuritic plaques was noted in 15-mo-old, vehicle-treated Tg2576 mice where CAA deposits had progressed to encompass almost the entire leptomeningeal arteriolar system without interruption (Fig. 2*A*). Importantly, apocynin treatment markedly reduced these CAA deposits, while having no effect on neuritic plaque deposits (Fig. 2*A*). To quantitate this in vivo observation, CAA and neuritic plaque loads were examined by subjecting fixed
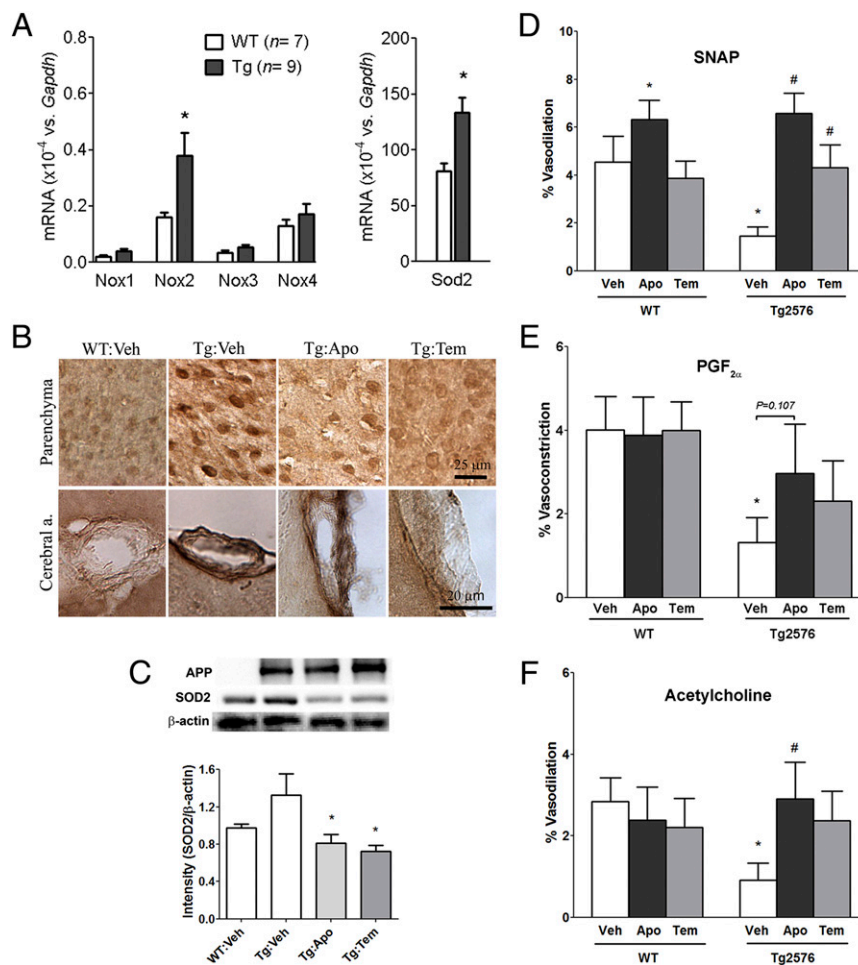
www.manaraa.com

Fig. 1. Apocynin and tempol attenuate oxidative stress and restores cerebrovascular dysfunction. (A) RNA extracted from leptomeningeal arteries of 12-mo-old Tg2576 and littermate WT mice was subjected to qPCR to compare transcript levels for Nox isoforms and Sod2, and calculated as relative expression to Gapdh gene. *$P < 0.05$ vs. WT mice. (B–F) Twelve-month-old Tg2576 and littermate WT mice were treated with apocynin (Apo), tempol (Tem), or vehicle (Veh) for 10–12 wk ($n = 5$–6). (B). Coronally sectioned brain tissues were subjected to immunolabeling with the oxidative stress marker anti–3-nitrotyrosine antibody. Elevated levels of 3-nitrotyrosine immunoreactivity were noted in neurons and cerebral vessel walls in the vehicle-treated Tg2576 mice. This immunoreactivity was attenuated in both apocynin- and tempol-treated Tg2576 mice. (C) Cortical tissue samples (30 μg per lane) were subjected to immunoblotting with a marker for oxidative stress, SOD2. Data indicate mean ± SEM, *$P < 0.05$ vs. vehicle-treated Tg2576 mice. (D–F) Live pial vessel responses to VSMC-dependent vasodilators SNAP (D) and constrictor PGF2α (E), and EC-dependent vasodilator acetylcholine (F) were assessed via closed cranial window and video microscopy. The percent change in vessel diameter was determined. Data indicate mean ± SEM; *$P < 0.05$ vs. WT:Veh group; #$P < 0.05$ vs. Tg2576:Veh group.

coronal brain sections to fluorescent double-labeling of fibrillar amyloid with resorufin and methoxy-X34 (Fig. 2B). We found that apocynin reduces CAA deposits by 80% (apocynin, 0.06 ± 0.02% vs. vehicle, 0.29 ± 0.08%; $P < 0.05$) while having no effect on neuritic plaque deposits (apocynin, 0.71 ± 0.13% vs. vehicle, 0.80 ± 0.08%; $P > 0.05$) (Fig. 2 C and D). A similar but non-significant selective decrease in CAA deposits was noted in tempol-treated animals (Fig. 2 C and D). These data indicate that anti-ROS therapy restores CV function in aged Tg2576 mice, at least in part, via selective reduction in CAA formation. This finding was unexpected and suggests that ROS contribute to the pathogenesis of CAA itself.

Apocynin and Tempol Reduce CAA-Induced Vasomotor Impairment. To determine whether anti-ROS therapy improves CV function in aged Tg2576 mice via additional mechanisms other than reducing CAA load, we examined CV function while controlling for CAA severity across individual vessel segments. To do so, vasodilatory responses in vehicle-treated, apocynin-treated, and tempol-treated aged Tg2576 mice were plotted against the percent CAA coverage

(Fig. 3 B and D) or against the presence or absence of CAA (Fig. 3 C and E). First, we documented that pial arteriole reactivity was significantly reduced in vessel segments with CAA vs. those without CAA in untreated aged Tg2576 mice (Fig. 3E) and that pial arteriole reactivity was completely abolished in vessel segments having greater than 20% CAA coverage in untreated aged Tg2576 mice (Fig. 3 B–D). Both of these findings are consistent with our previous report (13). Second, we found that apocynin significantly improved CV reactivity not only in vessel segments without CAA (Fig. 3E) or mild CAA (<20% coverage) (Fig. 3 B and D), but also in vessel segments having moderate CAA (21–60% coverage) (Fig. 3 B and D) and even severe CAA (>60% coverage) (Fig. 3B). We also found that tempol treatment restored CV reactivity in aged Tg2576 mice, albeit to a lesser degree (Fig. 3 B–E). The fact that apocynin and tempol improve CV function in vessel segments having such extensive CAA indicates that ROS-directed therapy is improving CV function not only via reduction in CAA formation but also by directly attenuating CAA-induced vasomotor impairment.
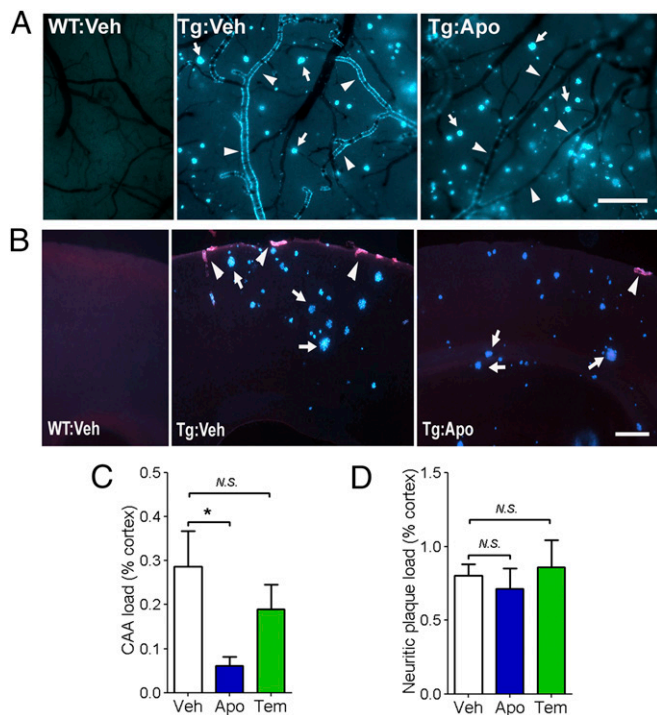
Fig. 2. Apocynin preferentially reduces CAA loads, but not parenchymal plaque loads in aged Tg2576 mice. Twelve-month-old Tg2576 and littermate WT mice were treated with apocynin (Apo), tempol (Tem), or vehicle (Veh) for 10–12 wk (n = 5–6). (A) Live imaging of amyloid deposition with methoxy-X04 staining demonstrated that amyloid deposition both in the pial vessels (arrowheads) and in the parenchymal tissues (arrows) were noted in vehicle-treated Tg2576 mice. There was a marked decrease in CAA load but not in plaque load in apocynin-treated mice. (B) Histological assessment in brain sections further confirmed that CAA loads (arrowheads in B) were significantly reduced by apocynin treatment, whereas parenchymal plaque loads (arrows in B) were not affected. (C and D) CAA was quantified by measuring percent coverage of resorufin-positive vessels in the cortex (C) whereas neuritic plaque load was calculated by subtracting CAA load from the total X04–positive amyloid load in the cortex (D). Data indicate mean ± SEM, *P < 0.05 by ANOVA.

Apocynin and Tempol Do Not Reduce CAA-Induced VSMC Loss. Another manner by which anti-ROS therapy could improve CAA-related CV dysfunction is by reducing CAA-induced VSMC toxicity. To investigate this possibility, we quantified VSMC density and CAA load in aged Tg2576 and littermate WT mice treated with vehicle, apocynin, or tempol using fluorescent labeling of CAA and VSMCs and multiphoton microscopy (Fig. S6). Similar to our previous report (13), we documented an overall loss of VSMC density in the leptomeningeal vessels of aged Tg2576 mice compared with littermate WT mice (Fig. 4A). We also found that apocynin significantly reduces this VSMC loss (P < 0.05) (Fig. 4A). However, when we controlled for CAA severity by examining VSMC density in vessel segments with similar degrees of CAA, apocynin treatment had no appreciable effect on VSMC loss (Fig. 4B). Similar results were seen in tempol-treated animals (Fig. 4B). These data indicate that ROS-directed interventions reduce VSMC loss in vessels of aged Tg2576 mice primarily by decreasing CAA load and not by reducing CAA-induced VSMC toxicity.

Apocynin Reduces CAA-Associated Microhemorrhage. Prussian blue staining has been widely used for detection of hemosiderin, a degradation product of hemoglobin captured in microglia/macrophages where microhemorrhages have occurred. We found that Prussian blue-positive microhemorrhages were present in aged

Tg2576 mice but not in WT mice (Fig. 5A). We also found that apocynin significantly reduces the number of microhemorrhages in aged Tg2576 mice (apocynin, 1.25 ± 0.4 vs. vehicle, 2.5 ± 0.4 profiles per section, P = 0.04) (Fig. 5B). A similar (but non-significant) reduction in the number of microhemorrhages was noted in tempol-treated animals (Fig. 5B). These data indicate that the decrease in CAA formation afforded by anti-ROS therapy produces an important reduction in CAA-related microhemorrhage.

Apocynin and Tempol Reduce Brain ApoE Levels. To begin to explore the mechanisms by which anti-ROS therapy selectively attenuates the development of CAA, we examined two factors known to strongly influence CAA pathogenesis: brain ApoE levels and brain $A\beta_{40}/A\beta_{42}$ ratio. To do so, apocynin (1.5 mM) was fed in drinking water for 12 wk to WT or Tg2576 mice beginning at 6 mo of age. This age (which precedes vascular and parenchymal amyloid deposition) was chosen to avoid the confound that amyloid plaques have on accurately quantitating soluble Aβ (42, 43). Aβ ELISAs demonstrated that apocynin did not affect the levels of $A\beta_{40}$ and $A\beta_{42}$ in cortex and cerebrospinal fluid (Fig. 6 A and B), nor did it affect $A\beta_{40}/A\beta_{42}$ ratios (Fig. 6C). In contrast, apocynin significantly reduced ApoE levels in the cortex (Fig. 6D). In a separate experiment, apocynin (1.5 mM) or tempol (1 mM) was fed in drinking water for 2 wk to Tg2576 mice beginning at 3 mo of age—an age that again precedes vascular and parenchymal amyloid deposition. Results from this experiment confirmed that apocynin significantly reduced brain ApoE levels and found that tempol also tends to reduce brain ApoE levels (Fig. S7). These data suggest that the manner by which apocynin and tempol reduce CAA formation is via its influence on brain ApoE metabolism.

Apocynin Reduces Inflammatory Activation of Astrocytes and Microglia in Aged Tg2576 Mice. We examined the effect of apocynin on astrocyte and microglial activation by performing GFAP and CD45 immunohistochemistry in aged Tg2576 mice. Consistent with previous reports (20, 44), we noted a marked increase in both GFAP- and CD45-positive immunoreactivities in aged Tg2576 mice (Fig. 7). We also found that apocynin treatment significantly reduced activated astrocytes and microglial cells by 40% and 45%, respectively, whereas tempol treatment had less effect on GFAP- and CD45-positive immunoreactivity (Fig. 7). Double labeling with methoxy-X34 and activated glial markers demonstrated that apocynin primarily reduces the number of activated astrocytes and microglial cells around methoxy-X34–positive (dense core) neuritic plaques (Fig. S8).

Discussion

Our study has several important findings. First, two different anti-ROS interventions—the NADPH oxidase inhibitor, apocynin, and the nonspecific ROS scavenger, tempol—reduce oxidative stress and improve CV function in aged Tg2576 mice. Second, the CV protection afforded by anti-ROS therapy was the product of both a decrease in CAA formation as well as a direct reduction in CAA-induced vasomotor impairment. Third, anti-ROS therapy decreases microhemorrhage—another important downstream consequence of CAA. Taken together, these findings represent direct evidence that ROS play a causal role in the CV deficits induced by fibrillar Aβ in the form of CAA and that the source of the ROS is likely NADPH oxidase. In addition, we provide preliminary evidence that one mechanism by which ROS impact CAA pathogenesis is via an effect on ApoE—a factor known to promote CAA formation (45, 46). Our findings have both mechanistic and therapeutic significance. For the former, our results provide strong and direct evidence that ROS are a key contributor to CAA-induced CV deficits and that they play a key role in CAA pathogenesis. For the latter, our results suggest
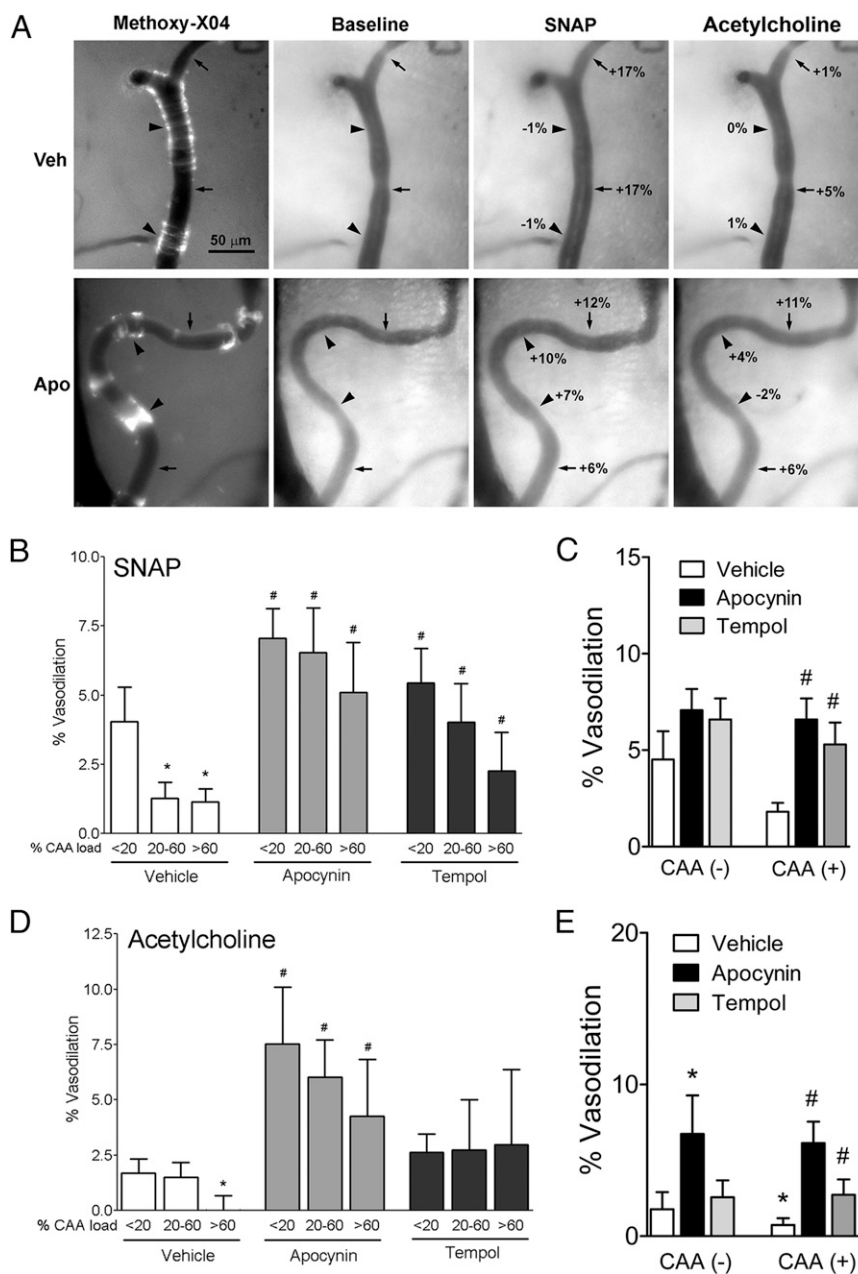
Fig. 3. Apocynin and tempol restore VSMC-dependent cerebrovascular dysfunction in CAA-affected vessels. Twelve-month-old Tg2576 and littermate WT mice were treated with apocynin, tempol or vehicle for 10–12 wk. Live pial vessel responses to VSMC-dependent vasodilator (SNAP) was assessed via closed cranial window and video microscopy. (*A*) Representative images of pial arteriolar responses to SNAP and acetylcholine in Tg2576 mice treated with vehicle or apocynin. In the vehicle-treated Tg2576 mice, vasodilatory responses were abolished in CAA-affected vessel segments (arrowheads) compared with CAA-free vessel segments (arrows). In the apocynin-treated Tg2576 mice, however, vasodilatory responses were apparent in both CAA-affected and CAA-free vessel segments. (*B* and *D*) Relationship between CAA coverage vs. vasodilatory responses to SNAP (*B*), and acetylcholine (*D*). Percentage of CAA coverage within 25-μm longitudinal vessels (eight consecutive segments per brain) was assessed as described in the *Methods*. Data indicate mean ± SEM; *$P < 0.05$ vs. vessel segments with <20% CAA load; #$P < 0.05$ vs. vehicle-treated group having corresponding % CAA coverage. (*C* and *E*) Vascular reactivity to SNAP (*C*) and acetylcholine (*E*) was also compared between vessel segments having CAA [CAA (+)] vs. those without CAA [CAA (−)]. Data indicate mean ± SEM; *$P < 0.05$ vs. vessel segments without CAA in vehicle-treated group; #$P < 0.05$ vs. vessel segments with CAA in vehicle-treated group.

that anti-ROS interventions such as NADPH oxidase inhibition carry great promise as a novel therapeutic approach for patients with CAA and AD.

CAA-Induced Vascular Dysfunction. Our results confirm our past findings (13) and past findings of others (27, 28, 47) that aged Tg2576 mice have substantial CV dysfunction. Moreover, they show that (*i*) the extent of this vascular impairment is dependent

on the presence and severity of CAA, and (*ii*) the nature of this CV impairment is fundamentally different from that of soluble Aβ-induced vessel dysfunction. Regarding the first assertion, our results demonstrate that vasomotor deficits in aged Tg2576 mice are greater in vessel segments having moderate-to-severe CAA vs. vessel segments having mild CAA. This finding is consistent with our past study (13), which was the first to report the association between CAA severity and extent of vessel dysfunction.
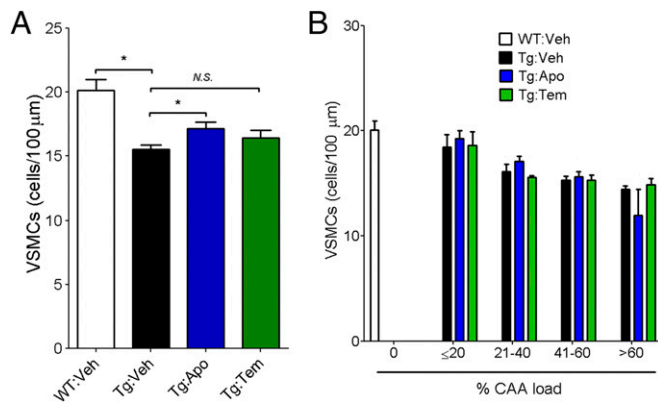
Han et al.

Fig. 4. Apocynin and tempol do not affect CAA-induced VSMC loss. Twelve-month-old Tg2576 and littermate WT mice were treated with apocynin (Apo), tempol (Tem), or vehicle (Veh) for 10–12 wk (n = 5–6). Amyloid deposition and VSMCs in leptomeningeal vessels were stained with methoxy-X04 and phalloidin-Alexa 488, respectively, and imaged with two-photon microscopy. (A) Number of VSMCs per 100-μm longitudinal vessel segment was counted. (B) Correlation between CAA severity and VSMC loss was plotted. Data indicate mean ± SEM; *P < 0.05 by ANOVA.

When coupled with the fact that CAA-ladened vessels are poorly responsive to soluble Aβ-directed interventions (13), these data strongly implicate CAA as having a causal role in the severe CV deficits noted in aged APP mice.

Regarding the second assertion, several lines of evidence indicate that there are fundamental differences between CAA-induced vs. soluble Aβ-induced CV dysfunction. First, CAA causes more severe CV deficits than soluble Aβ alone. Evidence for this notion stems from ex vivo (48) and in vivo (13) studies in which CV function was compared in young APP mice without CAA vs. aged APP mice with CAA. Second whereas soluble Aβ-induced CV deficits are primarily linked to EC dysfunction, CAA-induced CV deficits are predominantly the consequence of VSMC dysfunction. Evidence for the latter include: (*i*) CAA-ladened vessels from transgenic mice have reduced responses to EC-independent/VSMC-dependent vasoactive stimuli including hypercapnia (present study and refs. 13, 47, and 49), sodium nitroprusside (27), SNAP (present study and ref. 13), and PGF$_{2\alpha}$ (present study); and (*ii*) CAA-ladened vessels from transgenic mice and humans develop substantial VSMC disruption and degeneration in advanced stages of the disease (13, 50, 51). Third, although soluble Aβ induces a hypercontractile phenotype in which responses to vasodilators are reduced and responses to vasoconstrictors are exaggerated (15–19, 22, 26, 52, 53), CAA induces a hypocontractile vascular phenotype in which responses to vasodilators and vasoconstrictors are diminished. Evidence for the latter are as follows. Shin et al. (47) used laser speckle flowmetry to show that aged Tg2576 mice have reduced CBF responses to vasodilatory and vasoconstrictory stimuli. Dietrich et al. (48) used an isolated cerebral arteriole preparation to show that CAA-ladened vessels from aged Tg2576 mice have reduced responses to vasodilatory and vasoconstrictory stimuli. Our present study using a cranial window preparation in aged Tg2576 mice shows that CAA-ladened vessels have reduced responses to vasodilatory and vasoconstrictory stimuli.

In total, our present data, when coupled with past results, strongly support the notion that CAA causes a more severe and fundamentally different form of CV impairment compared with soluble Aβ. These differences may account, at least in part, for the established link between CAA and neurological morbidity due to ischemic stroke, cerebral hemorrhage, and dementia compared with soluble Aβ-induced CV dysfunction in which the

clinical consequences have yet to be established [for a review, see Zipfel et al. (54)]. It is therefore critical that the underlying mechanisms of CAA-induced CV impairment be determined.

Contribution of ROS to CAA-Induced Vascular Dysfunction. Most mechanistic studies examining the pathophysiological effects of Aβ on CV function have focused on soluble Aβ species, with the majority reporting that Aβ monomers (especially Aβ$_{40}$) cause a hypercontractile vascular phenotype potentiated by EC dysfunction (see discussion above). Several lines of evidence indicate that NADPH oxidase-derived ROS are responsible for these deficits. First, soluble Aβ causes vascular oxidative stress in a variety of experimental settings (29, 55). Second, pharmacologic and genetic inhibition of NADPH oxidase blocks the CBF deficits induced via topical application of synthetic Aβ$_{40}$ onto the cortical surface of live mice (23). Third, and most importantly, young Tg2576 mice with elevated endogenous Aβ monomers (but no CAA) lacking the NADPH oxidase subunit Nox2 do not develop significant CV dysfunction (28).

Whether ROS and, in particular, NADPH oxidase-derived ROS also contribute to CAA-induced CV deficits is poorly understood; however, three recent findings suggest this notion may be the case. First, Garcia-Alloza et al. (36) demonstrated that CAA-ladened vessels (but not CAA-free vessels) of aged Tg2576 mice develop severe oxidative stress. Second, Esposito et al. (37) noted that genetic knockdown of mitochondrial SOD2—which increases mitochondria-derived ROS—worsens CAA pathology in aged APP mice. Third, Park et al. (28, 35) found that aged Tg2576 mice treated with an NADPH oxidase peptide inhibitor develop less severe CV dysfunction and that aged Tg2576 mice lacking the NADPH oxidase subunit Nox2 develop no CV deficits at all. Although the presence of CAA and its effect on CV function were not examined in these studies, the fact that Tg2576 mice were assessed at an age when CAA is expected (28, 35)
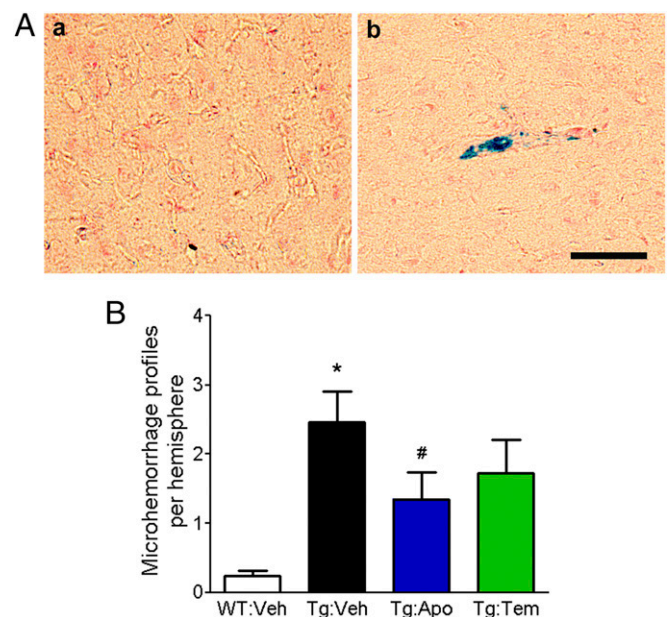

Fig. 5. Apocynin attenuates CAA-associated microhemorrhage in aged Tg2576 mice. Twelve-month-old Tg2576 and littermate WT mice were treated with apocynin (Apo), tempol (Tem), or vehicle (Veh) for 10–12 wk (n = 5–6). (A) Brain sections were subjected to Prussian blue staining to detect microhemorrhage (blue in color) and counterstaining with Nuclear Fast Red. Representative images from brain sections of WT mice (*a*) and aged Tg2576 mice (*b*) are seen. (B) Number of microhemorrhagic profiles per section was assessed. *P < 0.05 vs. WT:Veh group; #P < 0.05 vs. Tg2576:Veh group.
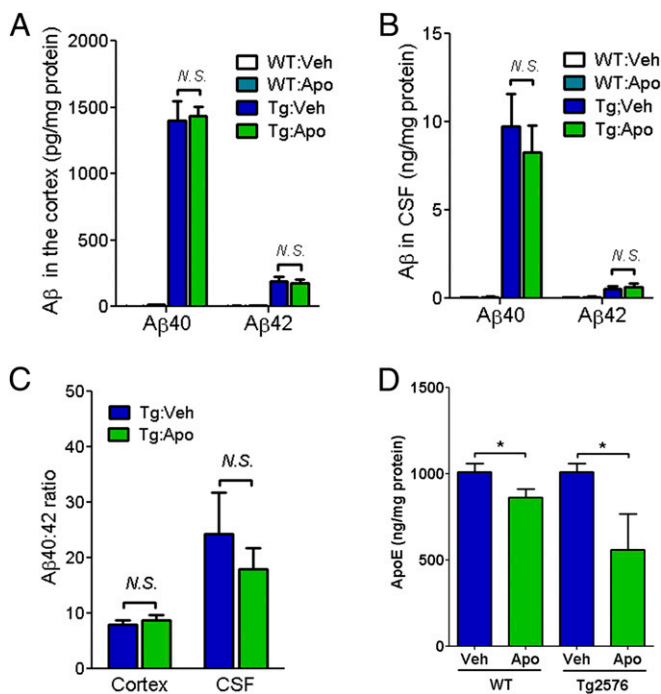
www.manaraa.com

Fig. 6. Effects of apocynin on levels of Aβ and ApoE in young mice. Six-month-old Tg2576 and littermate WT mice were treated with apocynin (Apo) or vehicle (Veh) for 12 wk ($n = 4$–6). Levels of $A\beta_{40}$ and $A\beta_{42}$ in the cortex (A) and CSF (B), ratio of $A\beta_{40}/A\beta_{42}$ (C), and levels of ApoE in the cortex (D) were determined by ELISAs. Data indicate mean ± SEM; *$P < 0.05$ by ANOVA.

suggests that ROS may play a causal role in CAA-induced CV impairment.

Results from the present study provide direct evidence that ROS are in fact a key mediator of CAA-induced CV deficits and strongly suggest that the source of this oxidative stress is NADPH oxidase. First, we demonstrated that the NADPH oxidase inhibitor, apocynin, and the nonspecific ROS scavenger, tempol, reduce oxidative stress and improve CV function in aged Tg2576 mice. Second, we showed that the source of the CV improvement is CAA-mediated because anti-ROS therapy reduces both CAA formation and CAA-induced vasomotor impairment. Third, we showed that anti-ROS therapy reduces microhemorrhage—another important consequence of CAA. These data not only confirm the studies of Park and coworkers, who were the first to show that the CV deficits in aged Tg2576 mice are ROS-mediated, but significantly extend them by shedding mechanistic insight into the manner by which ROS produce CV deficits (i.e., through promotion of CAA formation and CAA-induced vasomotor impairment). This insight was possible because we (*i*) histologically examined and quantified CAA, and (*ii*) assessed CV function in a way that permits direct quantification of CAA-induced vasomotor impairment. Importantly, although our results directly implicate ROS in CAA pathogenesis and CAA-induced CV deficits, additional experiments will be required to prove that NADPH oxidase is a key source of the offending ROS, given that some have reported that apocynin not only inhibits NADPH oxidase but may also function as a ROS scavenger (56, 57).

Role of ROS in CAA Pathogenesis. Several in vitro studies implicate oxidized cellular components in the promotion of Aβ fibrillization. Cholesterol oxidative metabolites modify Aβ peptides by Schiff base formation leading to spherical and fibrillar Aβ aggregates (58). Lipid oxidation products promote Aβ aggregation through a pathway involving modification of His residues in Aβ

proteins by Michael addition, leading to increased Aβ affinity for lipid membranes and heightened tendency for Aβ to aggregate into fibrils (59).

Multiple in vivo studies also implicate ROS in amyloid pathogenesis. Anti-ROS agents, including curcumin and phenyl-N-tert-butyl nitrene, reduce parenchymal amyloid burden in aged APP mice (60–63). Other anti-ROS agents, however, are not effective (20, 36, 64). Issues related to potency, specificity, and duration of therapy may have contributed these disparate results. Genetic approaches have also been used to examine the influence of ROS on amyloid formation. Three studies have examined the potential role of mitochondria-derived ROS: (*i*) Li et al. (65) noted that aged APP mice with heterozygous genetic knockdown of SOD2 (leading to greater mitochondria-derived ROS) develop an increase in parenchymal amyloid burden; (*ii*) Esposito et al. (37) reported that aged APP mice with genetic heterozygous knockdown of SOD2 (leading to greater mitochondria-derived ROS) develop a decrease in parenchymal amyloid burden (although neuritic dystrophy and neurobehavioral deficits were worse); and (*iii*) Massaad et al. (66) demonstrated that Tg2576 mice with genetic overexpression of SOD2 (leading to reduced mitochondria-derived ROS) develop a decrease in parenchymal amyloid burden and improved neurobehavioral outcome. Although somewhat contradictory in terms of the impact on amyloid load (increase vs. decrease), these results indicate that mitochondria-derived ROS play a key role in parenchymal plaque pathogenesis. In contrast, Iadecola and coworkers (28, 35) showed that NADPH oxidase-derived ROS play no apparent role in parenchymal amyloid pathogenesis because Tg2576 mice lacking Nox2 develop similar parenchymal plaque burden as littermate Tg2576 mice expressing WT Nox2. Overall, these pharmacologic and genetic studies strongly suggest that ROS play a contributing role in parenchymal amyloid pathogenesis and that
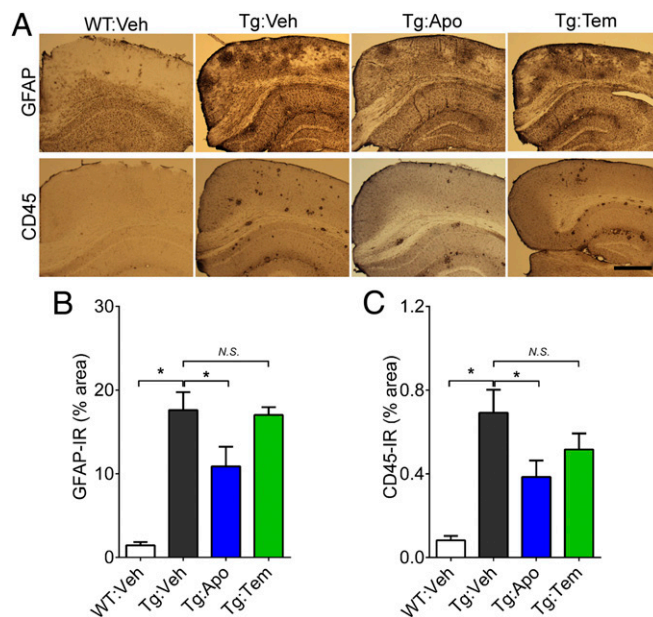
Fig. 7. Apocynin attenuates activation of astrocytes and microglia in aged Tg2576 mice. Twelve-month-old Tg2576 and littermate WT mice were treated with apocynin (Apo), tempol (Tem), or vehicle (Veh) for 10–12 wk. Activation of both astrocytes and microglia were noted in Tg2576 mice as determined by immunolabeling with cell type-specific markers for activated astrocytes (GFAP) and microglia (CD45) (A). Both GFAP- and CD45-positive immunoreactivity was significantly reduced in apocynin-treated Tg2576 mice ($n = 5$–6 per group) (B and C). *$P < 0.05$ as determined by ANOVA.

Han et al.

www.manaraa.com

mitochondria (rather than NADPH oxidase) are the principle source of the offending ROS.

The role of ROS in vascular amyloid pathogenesis, however, is less clear. Only three of the aforementioned pharmacologic studies and one of aforementioned genetic studies assessed the influence of ROS on CAA formation. Results from the pharmacological studies are as follows: (*i*) pomegranate juice (which has some antioxidant properties) administered to Tg2576 mice for 6 mo had no effect on CAA formation (63); (*ii*) curcumin (which has some antioxidant properties) administered to APP/PS1 dE9 mice for 7 d had a nonsignificant trend toward reducing CAA formation (62); and (*iii*) phenyl-*N-tert*-butyl nitrone (a nonspecific ROS scavenger) given to APP/PS1 dE9 and Tg2576 mice for 1 mo had no effect on CAA formation (36). Again, issues of potency, specificity, and duration of therapy could have affected these results. The result from the one genetic study is as follows: heterozygous genetic knockdown of SOD2 (leading to greater mitochondria-derived ROS) in APP mice led to an increase in vascular amyloid burden. In total, these four studies are less than conclusive in regard to the role of ROS in CAA pathogenesis, and the role of NADPH oxidase-derived ROS in CAA development has yet to be examined.

In the present study, we used the NADPH oxidase inhibitor, apocynin, and the nonspecific ROS scavenger, tempol, to directly determine the role of ROS in CAA formation. Both have well-documented potencies and selectivities for attenuating oxidative stress (56, 67, 68). In addition, the primary manner by which apocynin exerts its anti-ROS effect is via inhibition of NADPH oxidase—one of the two major ROS-producing pathways in cerebral vessels (the other being mitochondria) (32, 69). We found that 10–12 wk of apocynin treatment in aged Tg2576 mice reduces CAA formation by 80%, while having no significant effect on parenchymal plaque load. A trend for a similarly selective reduction in CAA formation was seen in aged Tg2576 mice treated with tempol. These data strongly implicate ROS and, in particular, NADPH oxidase-derived ROS in the pathogenesis of CAA. Moreover, our data offer a potential explanation for the findings of Iadecola and coworkers, who showed that genetic inhibition of NADPH oxidase improves CV function in aged Tg2576 mice (28)—that is, CAA formation may have been reduced and therefore contributed to the observed improvement in CV function. When coupled with the aforementioned genetic studies that implicate mitochondria-derived ROS in parenchymal amyloid pathogenesis, our data linking NADPH oxidase-derived ROS to CAA pathogenesis raises the intriguing possibility that the source of ROS may play a critical role in its influence on parenchymal vs. vascular amyloid deposition.

To explore the mechanisms by which vascular oxidative stress contributes to CAA pathogenesis, we examined the influence of apocynin on two factors known to influence the distribution of vascular vs. parenchymal amyloid—apolipoprotein E (ApoE) and the $A\beta_{40}/A\beta_{42}$ ratio. ApoE is an extracellular Aβ binding protein that influences Aβ fibrillogenesis and clearance. When ApoE is genetically deleted in Tg2576 mice, parenchymal amyloid deposits are modestly decreased and CAA is virtually eliminated (45). A fifty percent reduction of ApoE also decreased CAA (45). In contrast, when human ApoE4 is overexpressed in Tg2576 mice, the distribution of amyloid pathology is altered in favor of vascular vs. parenchymal deposits (46). In the present study, we found that apocynin and, to a lesser degree, tempol decrease mouse ApoE levels—an effect that would be expected to decrease CAA formation to a far greater extent than neuritic plaques. In addition, we examined the impact of apocynin on the $A\beta_{40}/A\beta_{42}$ ratio but found no significant effect. Taken together, our data suggest that the manner by which oxidative stress promotes CAA formation is via its influence on ApoE rather than any potential influence on Aβ metabolism. Additional experiments will be required to definitively

establish ApoE as the key factor and to determine the manner in which oxidative stress impacts ApoE metabolism.

Conclusion

Our work supports the findings of previous investigators who documented that ROS and, in particular, NADPH oxidase-derived ROS play a role in the severe CV deficits noted in aged Tg2576 mice. In addition, our results extend these past observations on several fronts. First, we provide direct evidence that ROS are responsible for CAA-induced CV dysfunction. Second, we show that ROS underlie CAA-related microhemorrhage. Third, we demonstrate two mechanisms by which oxidative stress contributes to CAA-induced CV deficits: (*i*) promotion of CAA formation, and (*ii*) direct induction of vasomotor impairment. Fourth, we provide strong evidence that the source of the offending ROS is NADPH oxidase–one of the two principle pathways by which oxidative stress is produced in cerebral vessels. Finally, we provide preliminary evidence that the mechanism by which ROS promote CAA formation is via the influence of ROS on brain ApoE levels. These data strongly suggest that ROS and, in particular, NADPH oxidase-derived ROS are a promising therapeutic target for CAA-related neurological morbidity including ischemic brain injury, cerebral hemorrhage, and AD and non-AD dementia. Whether other ROS producing pathways (in particular mitochondria) also contribute to CAA-induced CV deficits, whether CAA-directed therapies of any kind reduce ischemic brain injury and/or enhance cognitive function, and whether long-term anti-ROS therapy sufficient to positively impact CAA carries any significant side effects (e.g., immune suppression) are all important topics for future investigation.

Methods

Animals and Materials. All experimental protocols were approved by the Animal Studies Committee at Washington University. The production, genotyping, and background strain (B6/SJL) of Tg2576 mice used in this study have been described previously (42, 70). Tg2576 mice overexpress human APP695 with the familial Swedish AD mutations at positions 670/671 under control of the hamster prion protein (PrP) promoter and were a generous gift from K. Ashe (University of Minnesota, Minneapolis, MN). Apocynin and tempol were purchased from Sigma-Aldrich. PS1APP mice were also used in our study. These mice have a C57BL/6J genetic background that coexpresses KM670/671NL mutated APP and L166P mutated presenilin 1 under the control of a neuron-specific Thy1 promoter element (71).

Drug Administration. In one experiment, 12-mo-old Tg2576 mice and WT mice were treated with the NADPH oxidase inhibitor apocynin (1.5 mM) or the free radical scavenger tempol (1 mM) in drinking water for 10–12 wk (*n* = 5–6 per group). Drug treatment was initiated at 12 mo of age, when Tg2576 mice have substantial parenchymal plaque loads but limited CAA loads (13). In a second experiment, Tg2576 and WT mice were treated with apocynin (1.5 mM) in drinking water for 12 wk beginning at 6 mo of age (*n* = 6 per group) to determine whether apocynin influences Aβ levels, the $A\beta_{40}/A\beta_{42}$ ratio, and ApoE levels. In a third experiment, PS1APP mice were treated with apocynin (1.5 mM) or tempol (1mM) in drinking water for 2 wk beginning at 3 mo of age (*n* = 4–5 per group) to determine whether apocynin and tempol influence ApoE levels. Doses of apocynin and tempol were chosen according to previous reports (20, 72).

Closed Cranial Window Preparation and Live Microscopic Imaging. A closed cranial window preparation was performed as previously reported (13). Briefly, mice were anesthetized with isoflurane (4% induction, 1.5% maintenance), and a 4-mm-diameter craniotomy was performed with a water-cooled dental drill in the right parietal bone. Two silastic tubings (i.d., 0.3 mm; o.d., 0.64 mm; Dow Corning) were inserted through the bone wax to permit topical application of vasodilators. The craniotomy was filled artificial cerebrospinal fluid (aCSF) (in mM: 125 NaCl, 26 NaHCO3, 1.25 NaH2PO4, 2.5 KCl, 1 MgCl2, 1 CaCl2, and 25 glucose) and sealed to the bone with a microscope coverglass using dental cement. To label amyloid deposits in the brain, mice were i.p. injected with a Congo red derivative, methoxy-X04. Fifteen hours later, mice were reanesthetized with isoflurane and

α-chloralose and ventilated. An arterial catheter was placed into the femoral artery for measuring mean arterial blood pressure and arterial blood gas analysis. Each mouse was then placed in a custom-built stereotaxic device to secure its head on the microscope stage. Leptomeningeal vessels were visualized using a Nikon Eclipse 600ME digital video microscopy system. To induce hypercapnia, mice were ventilated with 5% CO_2/30% O_2-containing air for 5 min followed by ventilation with 30% O_2-containing air. For topical vasoactive agents, the EC-dependent vasodilator acetylcholine (100 μM), the EC-independent/VSMC-dependent vasodilator S-nitroso-N-acetyl-penicillamine (SNAP; 500 μM), or the EC-independent/VSMC-dependent vasoconstrictor PGF2α (10 μM) was infused into the cranial window at a rate of 20 μL/min for 5 min.

Statistical Analyses. Data were expressed as means ± SEM. Comparison among multiple groups was performed with a one-way analysis of variance (ANOVA) followed by Dunnett's multiple comparison method. A P value <0.05 was considered significant.

Additional materials and methods are available in *SI Methods*.

1. Revesz T, et al. (2002) Sporadic and familial cerebral amyloid angiopathies. *Brain Pathol* 12(3):343–357.
2. Mann DM, et al. (1996) Predominant deposition of amyloid-beta 42(43) in plaques in cases of Alzheimer's disease and hereditary cerebral hemorrhage associated with mutations in the amyloid precursor protein gene. *Am J Pathol* 148(4):1257–1266.
3. Sisodia SS (1999) Alzheimer's disease: Perspectives for the new millennium. *J Clin Invest* 104(9):1169–1170.
4. Selkoe DJ (2001) Alzheimer's disease: Genes, proteins, and therapy. *Physiol Rev* 81(2):741–766.
5. Maia LF, Mackenzie IR, Feldman HH (2007) Clinical phenotypes of cerebral amyloid angiopathy. *J Neurol Sci* 257(1-2):23–30.
6. Nicoll JA, Yamada M, Frackowiak J, Mazur-Kolecka B, Weller RO (2004) Cerebral amyloid angiopathy plays a direct role in the pathogenesis of Alzheimer's disease: Pro-CAA position statement. *Neurobiol Aging* 25(5):589–597; discussion 603–604.
7. Vinters HV (1987) Cerebral amyloid angiopathy: A critical review. *Stroke* 18(2):311–324.
8. Greenberg SM (2002) Cerebral amyloid angiopathy and vessel dysfunction. *Cerebrovasc Dis* 13(Suppl 2):42–47.
9. Okazaki H, Reagan TJ, Campbell RJ (1979) Clinicopathologic studies of primary cerebral amyloid angiopathy. *Mayo Clin Proc* 54(1):22–31.
10. Greenberg SM, Vonsattel JP, Stakes JW, Gruber M, Finklestein SP (1993) The clinical spectrum of cerebral amyloid angiopathy: Presentations without lobar hemorrhage. *Neurology* 43(10):2073–2079.
11. Vermeer SE, et al. (2003) Silent brain infarcts and the risk of dementia and cognitive decline. *N Engl J Med* 348(13):1215–1222.
12. Itoh Y, Yamada M (1997) Cerebral amyloid angiopathy in the elderly: The clinico-pathological features, pathogenesis, and risk factors. *J Med Dent Sci* 44(1):11–19.
13. Han BH, et al. (2008) Cerebrovascular dysfunction in amyloid precursor protein transgenic mice: Contribution of soluble and insoluble amyloid-beta peptide, partial restoration via gamma-secretase inhibition. *J Neurosci* 28(50):13542–13550.
14. Suo Z, Fang C, Crawford F, Mullan M (1997) Superoxide free radical and intracellular calcium mediate A beta(1-42) induced endothelial toxicity. *Brain Res* 762(1-2):144–152.
15. Niwa K, et al. (2001) A beta-peptides enhance vasoconstriction in cerebral circulation. *Am J Physiol Heart Circ Physiol* 281(6):H2417–H2424.
16. Price JM, Sutton ET, Hellermann A, Thomas T (1997) beta-Amyloid induces cerebrovascular endothelial dysfunction in the rat brain. *Neurol Res* 19(5):534–538.
17. Paris D, et al. (2000) Soluble beta-amyloid peptides mediate vasoactivity via activation of a pro-inflammatory pathway. *Neurobiol Aging* 21(2):183–197.
18. Paris D, et al. (1999) Inhibition of Alzheimer's beta-amyloid induced vasoactivity and proinflammatory response in microglia by a cGMP-dependent mechanism. *Exp Neurol* 157(1):211–221.
19. Tong XK, Nicolakakis N, Kocharyan A, Hamel E (2005) Vascular remodeling versus amyloid beta-induced oxidative stress in the cerebrovascular dysfunctions associated with Alzheimer's disease. *J Neurosci* 25(48):11165–11174.
20. Nicolakakis N, et al. (2008) Complete rescue of cerebrovascular function in aged Alzheimer's disease transgenic mice by antioxidants and pioglitazone, a peroxisome proliferator-activated receptor gamma agonist. *J Neurosci* 28(37):9287–9296.
21. Borchelt DR, et al. (1997) Accelerated amyloid deposition in the brains of transgenic mice coexpressing mutant presenilin 1 and amyloid precursor proteins. *Neuron* 19(4):939–945.
22. Price JM, Chi X, Hellermann G, Sutton ET (2001) Physiological levels of beta-amyloid induce cerebral vessel dysfunction and reduce endothelial nitric oxide production. *Neurol Res* 23(5):506–512.
23. Niwa K, Carlson GA, Iadecola C (2000) Exogenous A beta1-40 reproduces cerebrovascular alterations resulting from amyloid precursor protein overexpression in mice. *J Cereb Blood Flow Metab* 20(12):1659–1668.
24. Iadecola C, et al. (1999) SOD1 rescues cerebral endothelial dysfunction in mice overexpressing amyloid precursor protein. *Nat Neurosci* 2(2):157–161.
25. Niwa K, et al. (2000) Abeta 1-40-related reduction in functional hyperemia in mouse neocortex during somatosensory activation. *Proc Natl Acad Sci USA* 97(17):9735–9740.
26. Niwa K, Kazama K, Younkin SG, Carlson GA, Iadecola C (2002) Alterations in cerebral blood flow and glucose utilization in mice overexpressing the amyloid precursor protein. *Neurobiol Dis* 9(1):61–68.
27. Christie R, Yamada M, Moskowitz M, Hyman B (2001) Structural and functional disruption of vascular smooth muscle cells in a transgenic mouse model of amyloid angiopathy. *Am J Pathol* 158(3):1065–1071.
28. Park L, et al. (2008) Nox2-derived radicals contribute to neurovascular and behavioral dysfunction in mice overexpressing the amyloid precursor protein. *Proc Natl Acad Sci USA* 105(4):1347–1352.
29. Park L, et al. (2004) Abeta-induced vascular oxidative stress and attenuation of functional hyperemia in mouse somatosensory cortex. *J Cereb Blood Flow Metab* 24(3):334–342.
30. Park L, et al. (2005) NADPH-oxidase-derived reactive oxygen species mediate the cerebrovascular dysfunction induced by the amyloid beta peptide. *J Neurosci* 25(7):1769–1777.
31. Block ML (2008) NADPH oxidase as a therapeutic target in Alzheimer's disease. *BMC Neurosci* 9(Suppl 2):S8.
32. Brandes RP, Schröder K (2008) Differential vascular functions of Nox family NADPH oxidases. *Curr Opin Lipidol* 19(5):513–518.
33. Rivera J, Sobey CG, Walduck AK, Drummond GR (2010) Nox isoforms in vascular pathophysiology: Insights from transgenic and knockout mouse models. *Redox Rep* 15(2):50–63.
34. Iadecola C (2003) Cerebrovascular effects of amyloid-beta peptides: Mechanisms and implications for Alzheimer's dementia. *Cell Mol Neurobiol* 23(4-5):681–689.
35. Park L, Anrather J, Girouard H, Zhou P, Iadecola C (2007) Nox2-derived reactive oxygen species mediate neurovascular dysregulation in the aging mouse brain. *J Cereb Blood Flow Metab* 27(12):1908–1918.
36. Garcia-Alloza M, et al. (2009) Matrix metalloproteinase inhibition reduces oxidative stress associated with cerebral amyloid angiopathy in vivo in transgenic mice. *J Neurochem* 109(6):1636–1647.
37. Esposito L, et al. (2006) Reduction in mitochondrial superoxide dismutase modulates Alzheimer's disease-like pathology and accelerates the onset of behavioral changes in human amyloid precursor protein transgenic mice. *J Neurosci* 26(19):5167–5179.
38. Rodrigo J, et al. (2004) Nitric oxide in the cerebral cortex of amyloid-precursor protein (SW) Tg2576 transgenic mice. *Neuroscience* 128(1):73–89.
39. Trumbull KA, et al. (2012) Diapocynin and apocynin administration fails to significantly extend survival in G93A SOD1 ALS mice. *Neurobiol Dis* 45(1):137–144.
40. Brendza RP, et al. (2005) Anti-Abeta antibody treatment promotes the rapid recovery of amyloid-associated neuritic dystrophy in PDAPP transgenic mice. *J Clin Invest* 115(2):428–433.
41. Han BH, et al. (2011) Resorufin analogs preferentially bind cerebrovascular amyloid: Potential use as imaging ligands for cerebral amyloid angiopathy. *Mol Neurodegener* 6(1):86.
42. Hsiao K, et al. (1996) Correlative memory deficits, Abeta elevation, and amyloid plaques in transgenic mice. *Science* 274(5284):99–102.
43. Kawarabayashi T, et al. (2001) Age-dependent changes in brain, CSF, and plasma amyloid (beta) protein in the Tg2576 transgenic mouse model of Alzheimer's disease. *J Neurosci* 21(2):372–381.
44. Koenigsknecht-Talboo J, et al. (2008) Rapid microglial response around amyloid pathology after systemic anti-Abeta antibody administration in PDAPP mice. *J Neurosci* 28(52):14156–14164.
45. Fryer JD, et al. (2003) Apolipoprotein E markedly facilitates age-dependent cerebral amyloid angiopathy and spontaneous hemorrhage in amyloid precursor protein transgenic mice. *J Neurosci* 23(21):7889–7896.
46. Fryer JD, et al. (2005) Human apolipoprotein E4 alters the amyloid-beta 40:42 ratio and promotes the formation of cerebral amyloid angiopathy in an amyloid precursor protein transgenic model. *J Neurosci* 25(11):2803–2810.
47. Shin HK, et al. (2007) Age-dependent cerebrovascular dysfunction in a transgenic mouse model of cerebral amyloid angiopathy. *Brain* 130(Pt 9):2310–2319.
48. Dietrich HH, Xiang C, Han BH, Zipfel GJ, Holtzman DM (2010) Soluble amyloid-beta, effect on cerebral arteriolar regulation and vascular cells. *Mol Neurodegener* 5:15.
49. Dorr A, et al. (2012) Amyloid-β-dependent compromise of microvascular structure and function in a model of Alzheimer's disease. *Brain* 135(Pt 10):3039–3050.
50. Christie R, Kimchi E, Kajdasz S, Bacskai B, Hyman BT (2001) Multiphoton microscopy and amyloid angiopathy. *Amyloid* 8(Suppl 1):48–50.
51. Mandybur TI (1986) Cerebral amyloid angiopathy: The vascular pathology and complications. *J Neuropathol Exp Neurol* 45(1):79–90.
52. Thomas T, Thomas G, McLendon C, Sutton T, Mullan M (1996) Beta-amyloid-mediated vasoactivity and vascular endothelial damage. *Nature* 380(6570):168–171.
53. Thomas T, McLendon C, Sutton ET, Thomas G (1997) Cerebrovascular endothelial dysfunction mediated by beta-amyloid. *Neuroreport* 8(6):1387–1391.
54. Zipfel GJ, Han BH, Ford AL, Lee J-M (2009) Cerebral amyloid angiopathy: Progressive disruption of the neurovascular unit. *Stroke* 40(Suppl 3):S16–S19.
55. Gentile MT, et al. (2004) Mechanisms of soluble beta-amyloid impairment of endothelial function. *J Biol Chem* 279(46):48135–48142.
56. Stefanska J, Pawliczak R (2008) Apocynin: Molecular aptitudes. *Mediators Inflamm* 2008:106507.
57. Heumüller S, et al. (2008) Apocynin is not an inhibitor of vascular NADPH oxidases but an antioxidant. *Hypertension* 51(2):211–217.

Han et al.

58. Bieschke J, Zhang Q, Powers ET, Lerner RA, Kelly JW (2005) Oxidative metabolites accelerate Alzheimer's amyloidogenesis by a two-step mechanism, eliminating the requirement for nucleation. *Biochemistry* 44(13):4977–4983.

59. Liu L, Komatsu H, Murray IV, Axelsen PH (2008) Promotion of amyloid beta protein misfolding and fibrillogenesis by a lipid oxidation product. *J Mol Biol* 377(4): 1236–1250.

60. Sung S, et al. (2004) Modulation of nuclear factor-kappa B activity by indomethacin influences A beta levels but not A beta precursor protein metabolism in a model of Alzheimer's disease. *Am J Pathol* 165(6):2197–2206.

61. Yang F, et al. (2005) Curcumin inhibits formation of amyloid beta oligomers and fibrils, binds plaques, and reduces amyloid in vivo. *J Biol Chem* 280(7):5892–5901.

62. Garcia-Alloza M, Borrelli LA, Rozkalne A, Hyman BT, Bacskai BJ (2007) Curcumin labels amyloid pathology in vivo, disrupts existing plaques, and partially restores distorted neurites in an Alzheimer mouse model. *J Neurochem* 102(4):1095–1104.

63. Hartman RE, et al. (2006) Pomegranate juice decreases amyloid load and improves behavior in a mouse model of Alzheimer's disease. *Neurobiol Dis* 24(3):506–515.

64. Quinn J, et al. (2005) Chronic melatonin therapy fails to alter amyloid burden or oxidative damage in old Tg2576 mice: Implications for clinical trials. *Brain Res* 1037(1-2):209–213.

65. Li F, et al. (2004) Increased plaque burden in brains of APP mutant MnSOD heterozygous knockout mice. *J Neurochem* 89(5):1308–1312.

66. Massaad CA, Washington TM, Pautler RG, Klann E (2009) Overexpression of SOD-2 reduces hippocampal superoxide and prevents memory deficits in a mouse model of Alzheimer's disease. *Proc Natl Acad Sci USA* 106(32):13576–13581.

67. Zhang Y, et al. (2005) Apocynin but not allopurinol prevents and reverses adrenocorticotropic hormone-induced hypertension in the rat. *Am J Hypertens* 18(7):910–916.

68. Tang XN, Cairns B, Cairns N, Yenari MA (2008) Apocynin improves outcome in experimental stroke with a narrow dose range. *Neuroscience* 154(2):556–562.

69. Selemidis S, Sobey CG, Wingler K, Schmidt HH, Drummond GR (2008) NADPH oxidases in the vasculature: Molecular features, roles in disease and pharmacological inhibition. *Pharmacol Ther* 120(3):254–291.

70. Holtzman DM, et al. (2000) Apolipoprotein E facilitates neuritic and cerebrovascular plaque formation in an Alzheimer's disease model. *Ann Neurol* 47(6):739–747.

71. Radde R, et al. (2006) Abeta42-driven cerebral amyloidosis in transgenic mice reveals early and robust pathology. *EMBO Rep* 7(9):940–946.

72. Liu F, et al. (2009) Apocynin attenuates tubular apoptosis and tubulointerstitial fibrosis in transgenic mice independent of hypertension. *Kidney Int* 75(2):156–166.

www.manaraa.com